The stromal-vascular fraction of adipose tissue contributes to major differences between subcutaneous and visceral fat depots

Juan R. Peinado, Yolanda Jimenez-Gomez, Marina R. Pulido, Maria Ortega-Bellido, Cesar Diaz-López, Francisco J. Padillo, Jose López-Miranda, Rafael Vazquez-Martínez, Maria M. Malagon

Department of Cell Biology, Physiology and Immunology, University of Córdoba, (J.R.P., Y.J.-L., M.R.P., M.O.B, R.V.-M., M.M.M.); Instituto Maimónides de Investigación Biomédica (IMIBIC), University of Córdoba (J.R.P., Y.J.-L., M.R.P., M.O.B, J.L.M., R.V.-M., M.M.M.); CIBER Fisiopatología de la Obesidad y Nutrición (CIBEROBN), Instituto de Salud Carlos III (J.R.P., Y.J.-L., M.R.P., M.O.B, R.V.-M., M.M.M.); Department of General Surgery (C.D.-L., F.J.P.) and Lipid and Atherosclerosis Research Unit (J.L.M.), Reina Sofía University Hospital, Córdoba, Spain.

Brief title: *Proteomic dissection of fat depots (SAT vs. VAT)*

Address for correspondence: María M. Malagón. Department of Cell Biology, Physiology and Immunology. Campus Universitario de Rabanales. Edificio Severo/ Ochoa, Pl. 3. University of Córdoba. E-14014 Córdoba. Spain. Phone: +34 957 21 22 56. Fax: +34 957 21 86 34. E-mail: bc1mapom@uco.es

Disclosure Summary: The authors have nothing to disclose

Grant support: This work was supported by Ministerio de Ciencia e Innovación (MICINN)/FEDER (BFU2007-60180/BFI to MMM, FPU AP2005-3348 to MRP), Junta de Andalucía (CTS-03039, and BIO-0139 to MMM), and CIBER Obesidad y Nutrición (CIBERobn), Instituto de Salud Carlos III, Spain.

Keywords: Adipose tissue, lean, MALDI-TOF mass spectrometry, mature adipocytes, proteome, stromal-vascular fraction, 2D-PAGE.

We have identified proteins whose expression differs between visceral and subcutaneous adipose tissue and which may be implicated in the pathologies that differentially affect each fat depot.

Abstract

Adipose tissue represents a complex tissue both in terms of its cellular composition, as it includes mature adipocytes (MA) and the various cell types comprising the stromal-vascular fraction (SVF), and in relation to the distinct biochemical, morphological and functional characteristics according to its anatomical location. Herein, we have characterized the proteomic profile of both MA and SVF from human visceral (VAT) and subcutaneous (SAT) fat depots in order to unveil differences in the expression of proteins which may underlie the distinct association of VAT and SAT to several pathologies. Specifically, 24 proteins were observed to be differentially expressed between SAT SVF *vs.* VAT SVF from lean individuals. Immunoblotting and RT-PCR analysis confirmed the differential regulation of the nuclear envelope proteins Lamin A/C, the membrane-cytoskeletal linker ezrin and the enzyme involved in retinoic acid production, ALDH1A2, in the two fat depots. In sum, the observation that proteins with important cell functions are differentially distributed between VAT and SAT and their characterization as components of SVF or mature adipocytes, pave the way for future research on the molecular basis underlying diverse adipose tissue-related pathologies such as metabolic syndrome or lipodystrophy.

Introduction

Adipose tissue is a highly active metabolic tissue and important endocrine organ which, together with its classical role as energy storage depot, produces a wide variety of molecules with signaling properties (i.e. adipokines) that are involved in multiple functions including the regulation of metabolism, energy homeostasis, as well as immunity and inflammation (reviewed in (1). Far from being a simple organ, adipose tissue exhibits a marked heterogeneity both in terms of its cellular composition and in relation to its anatomical location. Thus, it is composed of mature adipocytes which are immersed in a complex collagen matrix wherein blood cells and preadipocytes coexist with nerve terminals and vascular tissue (2). These latter cellular components, comprising the stromal-vascular fraction (SVF), can be separated from mature adipocytes by enzymatic methods. This approach has enabled to show that adipokines are not only secreted by adipocytes but also by SVF cells (3), yet differences exist in the type and amount of molecules produced by each component. Accordingly, whereas adipokines such as leptin and adiponectin are primarily secreted by adipocytes (3), SVF cells contribute to most of the release of inflammatory mediators and interleukins such as Tumor Necrosis Factor-alpha (TNF-α) or interleukin-6 (IL-6) (4). These and other adipose-derived factors participate in the induction and maintenance of the subacute proinflammatory state associated with obesity that is commonly linked to the development of insulin resistance and type 2 diabetes (5).

In addition, the different adipose tissue depots exhibit unique adipokine expression and secretion profiles (for review (1). Importantly, VAT has been associated with increased risk for multiple morbidities including the metabolic syndrome (6) or type 2 diabetes (7). On the other hand, SAT is most highly associated with several cases of lipodystrophy, such as those related with several laminopathies (8).

By studying the proteome of mature adipocytes and the SVF of VAT and SAT, we have established the protein fingerprints of the different components of adipose tissue and showed that major differences between VAT and SAT can be attributed to the SVF proteome. Furthermore, in this scenario, we have identified proteins whose expression differs between the

two fat depots which may be related to the distinct pathologies associated to VAT or SAT such as metabolic syndrome or lipodystrophy.

Subjects and Methods

Subjects

The study was approved by the Ethical Committee of Reina Sofia Hospital (Córdoba, Spain) and all patients involved gave informed consent. Paired samples (7-8 g) of abdominal adipose tissue obtained from VAT and SAT of 14 Caucasian individuals (10 men and 4 women) undergoing elective open-abdominal surgery were collected between 9:00 and 11:00 AM. Subjects were 50 to 70 yr old with normal weight (Table 1). None of the individuals presented any chronic disease, diabetes, metabolic syndrome or altered biochemical parameters that could indicate adipose tissue alterations. Immediately after removal, biopsies were washed in DMEM (Invitrogen, Barcelona, Spain) and divided into 2-3 pieces, which were either frozen in liquid nitrogen and stored at -80ºC or processed for the separation of mature adipocytes and SVF.

Isolation of mature adipocytes and SVF

Freshly isolated SAT and VAT biopsies were collected in Krebs-Ringer Hepes medium (119 mM NaCl, 4.7 mM KCl, 1.2 mM $MgSO_4$, 2.5 mM $CaCl_2$, 1.2 mM KH_2PO_4, 20 mM Hepes pH 7.4, 2 mM glucose, 2% BSA) and washed twice to eliminate peripheral blood. Next, samples were incubated in Krebs-Ringer Hepes medium with 400 a.u./ml of collagenase (type V, Sigma, St Louis, MO) at 37ºC for 1 h in a shaking bath. Undigested tissue was removed by filtering through a sterile 100 µm pore Cell Strainer (BD Falcon, CA) and centrifuged at 600g for 10 min to separate the floating mature adipocyte layer from the pelleted SVF. Mature adipocytes were washed with DMEM, frozen in liquid nitrogen and stored at -80ºC. SVF was resuspended in DMEM, filtered through a 40 µm pore Cell Strainer and centrifuged at 400g for 5 min. Pelleted SVF was resuspended in 500 µl of erythrocyte lysis buffer (RBC Lysis Solution, Puregene, MN) and incubated for 3 min at RT. After centrifugation at 400 g for 10 min, SVF was frozen in liquid nitrogen and stored at -80ºC until protein extraction.

Protein extraction

Total adipose tissue and mature adipocytes were thawed in 0.4 ml of cold Urea/thiourea buffer [7 M urea, 2 M thiourea, 4% CHAPS, 45 mM Tris pH 7.4, 60 mM DTT, and complete protease inhibitors (1 tablet/20 ml, Roche, Barcelona, Spain)] supplemented with 0.1 mM NaCl. Cells were mechanically disrupted and briefly sonicated. Samples were adjusted to 900 µl with lysis buffer (20 mM Tris pH 7.4, 100 mM NaCl, 1% Triton and protease inhibitors) and incubated for 15 min at 35°C. After cooling on ice (10 min), 100 µl of 0.1 M Tris pH 7, and 50 mM $MgCl_2$ were added to the homogenates, which were then incubated with DNase I (30 U, Sigma) on ice (10 min). The homogenate was centrifuged (15 min, 10000g, 4°C) and the aqueous phase between the upper lipid phase and lower cellular debris phase was collected. Extensive delipidation was accomplished by Tri-n-butylphosphate-acetone-methanol precipitation (9). SVF was disrupted in 200 µl of lysis buffer. Extract was incubated with DNase I (30 U, Sigma) for 10 min in ice followed by standard chloroform/methanol precipitation. Precipitated proteins were resuspended in 75 µl of Urea/thiourea buffer. After Bradford assay for protein quantification, samples were diluted to 7 µg/µl with Urea/thiourea buffer and frozen at -20ºC.

Isoelectric focusing and 2D-PAGE

350 µg of protein from whole adipose tissue (n=3), mature adipocytes (n=3) and SVF (n=4) obtained from paired samples of SAT and VAT were diluted in 300 µl of Rehydratation Buffer and 0.8% of 3-10NL IPG buffer (GE Healthcare, Barcelona, Spain). Immobilized pH gradient strips (18cm, pH 3–10NL) were processed in an Ettan IPGPhor 3 System (GE Healthcare) following manufacturer instructions. Strips were equilibrated in SDS Equilibration Buffer [75 mM Tris, pH 8.8, 6 M urea, 30% glycerol, 2% SDS] containing 2% DTT for 15 min, followed by a 15-min wash with equilibration buffer containing 2.5% iodoacetamide. Proteins were separated on 12% Tris-glycine gels using an Ettan Dalt Six device (GE Healthcare), which resolved proteins with a MW higher than 20 kDa. Gels were stained with SYPRO Rubi dye and/or 0.1% Coomassie brilliant blue G-250, 10% ammonium sulfate, 2% phosphoric acid and 20% methanol.

MALDI-TOF-MS analysis

Spots were excised automatically in a ProPic station (Genomic Solutions, Huntingdon, UK) and subjected to MS analysis. For MALDI-TOF-MS analysis, gel specimens were distained twice (30 min, 37 °C) with 200 mM ammonium bicarbonate/40% acetonitrile. Gel pieces dehydrated for 5 min with pure acetonitrile and dried out over 4 h were automatically digested with trypsin according to standard protocols in a ProGest station (Genomic Solutions). MS and MS/MS analyses of peptides of each sample were analyzed in a 4,700 Proteomics Station (Applied Biosystems, CA).

Immunoblotting

Frozen samples from 4 additional individuals were disrupted in TBS buffer [20 mM Tris pH 7.4, 150 mM NaCl, 1% Triton and protease inhibitors] and incubated in the presence of DNase I (30 u; Sigma) on ice (15 min). 30-70 µg of protein were loaded on 10% SDS-PAGE and transferred to nitrocellulose membranes (Biotrace, Pall, Germany). After Ponceau staining to ensure equal sample loading, membranes were blocked for 1 h with 5% dried milk in TBS buffer with 0.05% Tween-20. After overnight incubation at 4ºC with the corresponding primary antibody, membranes were incubated with the appropriate IgG-HRP-conjugated secondary antibody. Immunoreactive bands were visualized with an enhanced-chemiluminescence reagent (Chemiluminescent HRP substrate, Millipore, MA). Optical densities of the immunoreactive bands were measured using ImageJ 1.40g software. Data were normalized to the corresponding β-actin band intensities.

Total RNA isolation and Real-Time PCR

Samples of VAT and SAT SVF obtained from at least 4 additional individuals were homogenized with an ULTRA-TURRAX T10 basic (IKA® Werke GmbH, Staufen, Germany) using TRIZOL® Reagent (Invitrogen). Total RNA samples were digested with RQ1 DNAse (Promega, Sydney, NSW) before RT-PCR. The expression levels of VAT-1 and ALDH1A2 genes, and of 18S ribosomal RNA (rRNA) as housekeeping gene, were measured by RT-PCR using an iCycler^{TM} Real-Time PCR System (Bio-Rad Laboratories, Hercules, CA). Specifically, 1 µg of total RNA underwent random primed reverse transcription using a First Strand cDNA

Synthesis kit (Fermentas, Burlington, ON, Canada). Real-Time PCR was carried out with 1 µl of cDNA and 24 µl of reaction mixture [12.5 µl of 2 x SYBR Green Supermix (Bio-Rad)], 9.5 µl of RNase-free water and 1 µl of the corresponding primers [VAT-1: sense, TCCTCTTTGACTTCGGCAAC; antisense, TGTGACCCCATTCTCCTTCA, ALDH1A2: sense, CAGTGTGGAGAAGGATGGATG; antisense, GCCTGCGTAATATCGAAAGGT, and 18S: sense, CCCATTCGAACGTCTGCCCTATC; antisense, TGCTGCCTTCCTTGGATGTGGTA]. After an initial hold of 2 min at 94ºC, samples were cycled 40 times at 94 ºC for 15 s and at 61 ºC for 15 s. For quantitative analysis, standard curve based method for relative Real-Time PCR data processing was utilized. The expression of each target gene was normalized to that of the housekeeping gene. All measurements were performed in duplicate. Controls consisting of reaction mixture without cDNA were negative in all runs.

Data analysis

2-D gel analysis was performed by PDQuest software (Bio-Rad), version 8.0. In order to reduce false positives, only those proteins with consistent differences of more than 1.5 times between samples were included in the analysis. Manual corrections were also performed to validate the matches automatically generated by the software. Spot volume values were normalized in each gel by dividing the raw quantity of each spot by the total volume of all the spots included in the same gel. Other normalizations provided by the PDQuest software were also performed with similar results. Variations of all the identified spots were finally confirmed and quantified by density measurements using ImageJ 1.40g software.

Statistical analysis used SSPS statistical software, version 11.0 for WINDOWS (SSPS INC., Chicago, IL). Normal distribution of variables to characterize differences in the expression of proteins under study was assessed using the Kolmogorov-Smirnov Test followed by a Student´s T test for independent samples. Differences were considered significant at $P < 0.05$. All data are expressed as mean ± S.E.M.

Results

Comparative 2D electrophoresis

Approximately 800 spots were observed in the gels prepared from whole adipose tissue extracts and from the separate fractions (mature adipocytes and SVF) of VAT and SAT (Figs. 1 and 2). Irrespective of the fat depot, analysis of the master gel obtained with the integrated proteome of mature adipocytes and SVF revealed that both subsets shared nearly 60% of the total number of spots detected. The remaining 40% of the spots corresponds to proteins exclusively present in the proteome of mature adipocytes (21%) or in that of SVF (19%).

Comparative proteomic analysis of mature adipocytes from VAT and SAT of lean individuals revealed the lack of consistent differences between them (Fig. 1B). This pattern was reproducible in the three distinct pairs of samples analyzed. In contrast, analysis of all spots present in the four distinct proteomes from paired visceral and subcutaneous SVF included in this study revealed 24 spots that were significantly different in SAT SVF *vs.* VAT SVF (Fig. 2). Of these, 17 were up-regulated and 7 were down-regulated in SVF from VAT *vs.* SAT (Table 2). The identified proteins could be grouped into the following categories: i) molecular chaperones and stress response (HSP70, chaperonin containing TCP1, and hSP56), ii) metabolism (3-phosphoglycerate dehydrogenase), ii) cytoskeleton and cell membrane-related events (cytokeratins KRT7, 8, 18, 19, coronin, ezrin, annexins A5, A7, A9 and A3, lamin A/C), iii) transport (transferrin), iv) adipose-derived hormones (visfatin, omentin), and v) redox state [aldehyde dehydrogenase A1 (ALDH1A1) and A2 (ALDH1A2), vesicle amine transport protein 1 (VAT-1)]. Among these proteins, only ezrin, hSP56, ALDHA1A1, KRT7, KRT8, KRT18, and KRT19 were also observed to be differentially expressed when the proteomes of whole VAT and SAT were compared (Fig. 1 and Supplemental Table 1). However, differences in the relative abundance of these proteins were more evident in SVF proteomes than in the proteomes of whole tissue extracts, as shown for ANXA5, hSP56 and KRT18 in Fig. 3. On the other hand, when the proteomes of whole VAT and SAT were compared, we could identify several differentially expressed proteins that were not detected in the analysis of the proteomic maps of the separate SVF. These included additional cytoskeletal proteins (*i.e.*, caldesmon 1, β-tropomyosin, and desmin, up-regulated in VAT; gelsolin, up-regulated in SAT), the chaperone

HSP27 (up-regulated in VAT) and gamma and beta fibrinogen (Fig. 1 and Supplemental Table 1).

Western Blot analysis of Lamin A/C and Ezrin

One protein overexpressed in the SVF of each depot was chosen for confirmation by western blot, one preferentially expressed in SAT, lamin A/C, and one more abundant in VAT, ezrin. As shown in Fig. 4A, two distinct immunoreactive bands were revealed using the anti-lamin A/C antiserum, corresponding to lamin A (74 kDa) and lamin C (65 kDa), in both VAT SVF and SAT SVF. Quantification of the immunoreactive bands confirmed up-regulation of both lamin A (1.34 fold) and lamin C (1.53 fold) in SAT SVF. Conversely, ezrin was up-regulated (3 fold) in VAT SVF (Fig. 4B).

Expression of VAT-1 and ALDH1A2 mRNA

Up-regulation of VAT-1 (2.2 fold) in SAT SVF and of ALDH1A2 (12.0 fold) in VAT SVF were documented with RT-PCR (Fig. 5).

Discussion

Over the last years, an increasing number of studies have focused on the analysis of the differences in the transcriptome, proteome and secretome between SAT and VAT [reviewed in (10), (11)], given their distinct characteristics regarding, among others, adipokine production, metabolic activity, proliferative capacity, apoptotic rate or adipocyte size, as well as their differential contribution for the development of various diseases (6, 12, 13). However, most of these studies were performed on whole adipose tissue preparations and only a few number employed human samples (14-16). Herein, we report for the first time the proteomes of isolated adipocytes and SVF from human VAT and SAT.

Our results showed that the protein fingerprints of isolated adipocytes from VAT and SAT of lean individuals were strikingly similar whereas significant differences were observed between the SVF of both fat depots in terms of their protein expression patterns. We have to include the caveat that, due to the technical limitations imposed by the high lipid content of adipocytes and/or to possible alterations induced by the cell separation protocol, our analysis

has likely skipped low represented or specific proteins that might be differentially expressed by isolated adipocytes. We are currently developing more sensitive approaches (DIGE and iTRAQ technologies) that will hopefully help to further explore the proteome of adipose tissue components. Notwithstanding these limitations, a recent cDNA microarray analysis of whole adipose tissue samples from omental and subcutaneous depots of lean to mildly obese individuals revealed that genes showing greater differential expression between the two depots were essentially expressed by the non-adipocyte component of adipose tissue. Although, as reported by the authors, some blood contamination remained in their samples, in our study all traces of blood were removed during the isolation of SVF, thus assuring that differences are to be ascribed to the stromal vascular components. Together, these findings support the notion that SVF contributes to major differences between VAT and SAT, at least in lean individuals, which highlights the relevance of this component to maintain the distinct identity of each fat depot.

Analysis of SVF from SAT and VAT confirmed variations in several proteins identified in a recent comparative proteomic study of whole VAT and SAT from obese subjects (16). These include up-regulation of ANXA5 in SAT and of hSP56, ALDH1A1, and KRT7, 8, 18 and 19 in VAT, thus pointing out the usefulness of these proteins as selective markers of each fat depot and, in particular, of their corresponding non-adipocyte fraction. Given that these proteins were observed to vary between SAT and VAT both in lean (our study) and obese individuals (16), it seems reasonable to propose that depot-specific differences in these proteins do not contribute significantly to the distinct functional behavior of the two fat pads with regards to obesity and related disorders.

The SVF of adipose tissue expresses several adipokines involved in the regulation of insulin action, including omentin and visfatin (18, 19). Accordingly, our proteomic analysis confirmed the presence of these two adipokines in SVF, both being more abundant in VAT than in SAT. In this regard, while the selective expression of omentin in VAT SVF has been clearly established (20), controversial results supporting either enrichment of visfatin mRNA in VAT (18) or similar mRNA expression levels in VAT and SAT (21) have been reported. Discrepancies

between these reports and our study could be accounted for by the occurrence of differences between visfatin transcript and protein levels. Nevertheless, it is worthy to mention that, in contrast to that revealed by the analysis of the separate fractions, we observed no differences in visfatin protein content when the proteomes of whole VAT and SAT were compared. Together, these observations indicate that analysis of the separate fractions may be critical for the identification of differentially expressed proteins between VAT and SAT. In this scenario, a key finding of our study has been the identification of the nuclear envelope proteins lamin A and C (lamin A/C), which we found overexpressed in SAT SVF. Mutations in the gene encoding lamin A/C (LMNA) or its processing enzymes have been described linked to inherited partial lipodystrophies (i.e., Dunnigan-type familial partial lipodystrophy, FPLD), which are characterized by loss of subcutaneous fat and excess intraabdominal fat as well as insulin resistance, type 2 diabetes, dyslipidemia and hepatic steatosis (22). Accordingly, obese and type 2 diabetes patients exhibit altered mRNA levels of lamin A/C in SAT (23). The higher expression of lamin A/C in SAT SVF *vs.* VAT SVF demonstrated herein is in contrast to that found in isolated adipocytes from human omental and subcutaneous fat, which show no differences in protein expression of the two lamins (24). Interestingly, transgenic mice expressing a mutated form of LMNA in adipose tissue, which exhibit many of the features of human FPLD, show fully functional mature adipocytes whereas preadipocytes are unable to differentiate into mature adipocytes (25), thus pointing out the relevance of lamin in normal functioning of preadipocytes. Indeed, a role for lamin A/C in adipocyte differentiation has been suggested based on its ability to associate with the adipocyte differentiation factor, sterol response element binding protein 1 (SREBP1) (26). In all, these data and our findings support the view that the preferential expression of lamin A/C in SAT, specifically in SVF preadipocytes of this depot, may contribute to the higher susceptibility of SAT to laminopathy-associated lipodystrophies when compared to VAT.

Besides lamin A/C, other proteins related to cellular structure and cytoskeleton were also differentially expressed in SVF of VAT and SAT. Of particular interest is ezrin, a member of the ERM (Ezrin/Radixin/Moesin) family which acts as membrane-cytoskeletal linker regulating

306 cortical morphogenesis and cell adhesion (27). These proteins, which are expressed in
307 endothelial cells (28), have been demonstrated to play a role in the adhesion of leukocytes to the
308 endothelium (28), and to mediate TNF-α-induced increases in both endothelial permeability
309 (29) and monocyte transmigratory activity (30). In this scenario, the observation that ezrin is
310 highly expressed in VAT SVF raises the possibility that this protein may be related to the
311 increased numbers of lymphocytes observed in visceral when compared to subcutaneous human
312 adipose tissue (31, 32) as well as to the preferential macrophage infiltration into VAT *vs.* SAT
313 observed in lean individuals and that has been shown to be exaggerated by central adiposity (32,
314 33). Given the demonstrated involvement of macrophages (34) and more recently, also of
315 lymphocytes (35), in the initiation and propagation of adipose tissue inflammation as well as in
316 the development of insulin resistance, it is conceivable that enhanced ezrin expression in VAT
317 SVF might underlie, at least in part, the increased clinical morbidity and differences in
318 metabolism in VAT relative to SAT.

319 In addition to ezrin, our study has enabled identification of other proteins whose expression
320 in adipose tissue has not been documented previously. This is the case of VAT-1, a synaptic
321 vesicle membrane protein widely expressed in the CNS and thought to be involved in nerve
322 signal transmission (36). Herein, we have shown that both VAT-1 mRNA and protein are
323 present in human adipose tissue, which demonstrates that VAT-1 is also expressed in peripheral
324 organs and, specifically, in fat SVF. Whether VAT-1 is a protein component of the autonomic
325 nervous system innervating adipose tissue remains to be determined. Nevertheless, its
326 differential expression in VAT *vs.* SAT SVF could reflect the dissimilar distribution of motor
327 afferent nerves and/or of the sensory innervation conveying information from adipose tissue to
328 the brain that has been depicted for the two fat pads (37).

329 Our study has enabled to confirm at proteomic scale previous transcriptomic data in mice on
330 the higher expression of the enzyme ALDH1A1 in VAT preadipocytes in comparison to their
331 counterparts from SAT (11). In addition, we also observed up-regulation of the isozyme
332 ALDH1A2 in VAT SVF at mRNA and protein levels. These two enzymes catalyze the
333 oxidation of the retinol metabolite, retinal, to retinoic acid (RA) (38). Together, these findings

support the view that VAT preadipocytes may produce higher levels of RA than SAT preadipocytes. In view of the demonstrated effects of RA on adipogenesis (39), it is conceivable that distinct depot-specific RA production underlies the differential capacity for differentiation exhibited by visceral and subcutaneous preadipocytes (40, 41).

In sum, we have characterized for the first time the proteome of the two fractions that compose adipose tissue, SVF and mature adipocytes, from lean individuals, thus broadening the current knowledge on the protein map of human adipose tissue. Furthermore, comparison of visceral and subcutaneous fat depot proteomes has allowed us to discover differentially expressed proteins which could represent new adipose markers of adipose-related pathologies that affect unevenly to the different fat depots, such as visceral obesity and associated metabolic syndrome derived disorders or several forms of lipodistrophy that mainly affect to SAT.

Acknowledgements

Mass spectrometry was performed at the Proteomics Facility (SCAI) of the University of Córdoba, which is Node 6 of the ProteoRed Consortium financed by Genoma España and belongs to the Andalusian Platform for Genomics, Proteomics and Bioinformatics. Antibodies against human lamin A/C and ezrin were kindly provided by Dr. Carlos Lopez-Otín (Univ. Oviedo, Spain) and Dr. Francisco Sánchez-Madrid (Hospital Universitario de la Princesa, Madrid, Spain), respectively.

Table 1 Biometric parameters of the individuals included in the study

n	14
Age (years)	56 ± 13
Weight (Kg)	66.6 ± 16
Height (cm)	170 ± 7
BMI (Kg/m^2)	22.8 ± 2.1
Glucose (mmol/l)	6.0 ± 0.2
Total cholesterol (mmol/l)	5.36 ± 0.6
Triglycerides (mmol/l)	1.61 ± 0.3
Insulin (μU/ml)	9.67 ± 0.4

Data are means ± SD

375 **Table 2**

Proteins identified by MALDI-TOF/TOF significantly increased in SVF of VAT vs. SAT									
Spot number	Mean fold change [a]	Protein name	Symbol	Accession number	MW (KDa)	pI	Pep. Count [b]	Total Ion Score[b]	*P value*[c]
1	4.08	Ezrin	EZR	NP_003370	69.5	5.94	20	130	0.0119
2	1.80	Transferrin	TF	AAB22049	77.0	6.85	42	503	0.0249
3	7.58	Aldehyde dehydrogenase 1 family, member A2	ALDH1A2	BAA34785	56.7	5.84	17	347	0.0251
4	1.53	Coronin, actin binding protein, 1A	CORO1A	NP_009005	51.7	6.12	13	85	0.0409
5	1.88	Nicotinamide phosphoribosyltransferase	VISFATIN	NP_005737	55.7	6.69	12	142	0.0494
6	5.79	Keratin 7[d]	KRT7	AAH02700	51.4	5.42	25	398	0.0345
7	2.98	Aldehyde dehydrogenase 1 family, member A1	ALDH1A1	AAC51652	55.4	6.30	10	89	0.0243
8	3.35	Keratin 8 [d]	KRT8	AAH73760	53.8	5.52	34	612	0.0297
9	3.98	Phosphoglycerate dehydrogenase	PHGDH	AAD51415	57.4	6.29	12	175	0.0086
10	2.54	Aldehyde dehydrogenase 1 family, member B1	ALDH1B1	P30837	57.7	6.36	15	300	0.0211
11	3.99	Selenium binding protein 1 [d]	hSP56	NP_003935	52.9	5.93	19	189	0.0386
12	5.22	Keratin 18 [d]	KRT18	CAA31377	47.3	5.27	27	422	0.0083
13	3.44	Annexin A7	ANXA7	BAD96272	50.5	6.77	15	131	ND
14	7.13	Keratin 19 [d]	KRT19	NP_002267	44.1	5.04	32	609	0.0034
15	3.50	Intelectin 1 (Omentin)	ITLN1	AAS49907	35.5	5.66	7	261	0.0480
16	1.92	Annexin A9	ANXA9	NP_003559	38.6	5.53	18	138	0.0103
17	2.60	Annexin A3	ANXA3	NP_005130	36.5	5.63	19	708	0.0163

Table 2b

Proteins identified by MALDI-TOF/TOF significantly increased in SVF of SAT vs. VAT									
Spot number	Mean fold change[a]	Protein name	Symbol	Accession number	MW (KDa)	pI	Pep. Count [b]	Total Ion Score[b]	*P value*[c]
1	1.86	Collagen, type VI, alpha 1	COL6A1	NP_001839	109.6	5.26	17	346	0.0101
2	2.02	Lamin A/C	LMNA	NP_005563	65.2	6.40	15	97	0.0463
3	1.81	Chaperonin containing TCP1, subunit 8	TCP-1-theta	BAB43952	59.3	5.70	10	86	ND
4	1.98	Vesicle amine transport protein 1 homolog	VAT-1	NP_006364	41.7	6.17	14	209	0.0450
5	3.75	Heat shock 70kDa protein 1A	HSP70.1	BAD93055	78.0	5.97	19	281	0.0079
6	1.90	Carbonic anhydrase I	CA1	NP_001729	28.9	6.59	14	779	0.0410
7	1.60	Annexin A5 [d]	ANXA5	AAH01429	35.8	4.94	21	701	0.0341

Spot numbers correspond to those on Fig. 2.

[a] Mean fold change indicates the average volume ratio (Visceral *vs.* Subcutaneous) of four independent individuals.

[b] Pep. count and Total Ion score values correspond to Mascot scores.

[c] P-value of Student's t-test; $P < 0.05$.

[d] Proteins also identified as differentially expressed in the same fat depot in the proteome of whole adipose tissue.

ND, Differences in these proteins were observed only in two out of the four SVF proteomes analyzed.

388

389 **Figures**

390 **Fig. 1** 2D-PAGE of whole adipose tissue (upper panels) and isolated mature adipocytes
391 (lower panels) of VAT (left panels) and SAT (right panels) from one individual.
392 Proteins were separated on a 2-DE gel using 18 cm pH 3-10 NL strips in the first
393 dimension and 12% SDS-PAGE gels in the second dimension, as described in Research
394 Design and Methods. Molecular weight standards were loaded on the second dimension
395 (right). Differentially expressed proteins between the two adipose tissue depots are
396 indicated with arrows. The numbers correspond to the spot numbers in supplemental
397 Table 1.

398 **Fig. 2** Characterization of the proteome of VAT and SAT SVF. A) Representative 2D-
399 PAGE of paired samples of VAT (left panel) and SAT (right panel) SVF from one
400 individual. Proteins with significant up-regulation in each fat depot are indicated by
401 arrows. The numbers correspond to the spot numbers in Table 2. B) Magnification of
402 the boxed region of the 2D-PAGE gels showing 5 proteins with higher expression in
403 either VAT SVF (PHGDH, Ezrin and ANXA3) or SAT SVF (Lamin A/C and VAT-1)
404 from two different individuals (Ind1 and 2).

405 **Fig. 3** A) Representative image of the proteome region that contains KRT18, HSP70
406 and ANXA5 (MW: 35-45 kDa and pI: 4.9-5.4) in whole adipose tissue, SVF and mature
407 adipocytes of VAT and SAT. B) Quantification of their relative abundance in whole
408 adipose tissue (n=3), SVF (n=4) and mature adipocytes (n=3) of both fat depots. * $P <$
409 0.05. V- (Visceral), S- (subcutaneous).

410 **Fig. 4** Protein abundance (by Western blot) of Lamin A/C (A) and Ezrin (B) in SVF
411 from VAT and SAT. The results were normalized for β-actin density. * $P < 0.05$,
412 (±S.E.M.). SVF from 4 individuals were used for these studies. Insets show
413 representative Western blots.

414 **Fig. 5** Mean (±S.E.M.) mRNA levels of VAT-1 (A; n=6) and ALDH1A2 (B; n=4) in
415 SVF of VAT and SAT. Results are expressed in arbitrary units. * $P < 0.05$.

References

1. **Kershaw EE, Flier JS** 2004 Adipose tissue as an endocrine organ. J Clin Endocrinol Metab 89:2548-2556
2. **Frayn KN, Karpe F, Fielding BA, Macdonald IA, Coppack SW** 2003 Integrative physiology of human adipose tissue. Int J Obes Relat Metab Disord 27:875-888
3. **Fain JN, Madan AK, Hiler ML, Cheema P, Bahouth SW** 2004 Comparison of the release of adipokines by adipose tissue, adipose tissue matrix, and adipocytes from visceral and subcutaneous abdominal adipose tissues of obese humans. Endocrinology 145:2273-2282
4. **Zeyda M, Farmer D, Todoric J, Aszmann O, Speiser M, Gyori G, Zlabinger GJ, Stulnig TM** 2007 Human adipose tissue macrophages are of an anti-inflammatory phenotype but capable of excessive pro-inflammatory mediator production. Int J Obes (Lond) 31:1420-1428
5. **Shoelson SE, Lee J, Goldfine AB** 2006 Inflammation and insulin resistance. J Clin Invest 116:1793-1801
6. **Wajchenberg BL, Giannella-Neto D, da Silva ME, Santos RF** 2002 Depot-specific hormonal characteristics of subcutaneous and visceral adipose tissue and their relation to the metabolic syndrome. Horm Metab Res 34:616-621
7. **Hamdy O, Porramatikul S, Al-Ozairi E** 2006 Metabolic obesity: the paradox between visceral and subcutaneous fat. Curr Diabetes Rev 2:367-373
8. **Araujo-Vilar D, Lattanzi G, Gonzalez-Mendez B, Costa-Freitas AT, Prieto D, Columbaro M, Mattioli E, Victoria B, Martinez-Sanchez N, Ramazanova A, Fraga M, Beiras A, Forteza J, Dominguez-Gerpe L, Calvo C, Lado-Abeal J** 2009 Site-dependent differences in both prelamin A and adipogenic genes in subcutaneous adipose tissue of patients with type 2 familial partial lipodystrophy. J Med Genet 46:40-48
9. **Mastro R, Hall M** 1999 Protein delipidation and precipitation by tri-n-butylphosphate, acetone, and methanol treatment for isoelectric focusing and two-dimensional gel electrophoresis. Anal Biochem 273:313-315
10. **Chen X, Hess S** 2008 Adipose proteome analysis: focus on mediators of insulin resistance. Expert Rev Proteomics 5:827-839
11. **Gesta S, Bluher M, Yamamoto Y, Norris AW, Berndt J, Kralisch S, Boucher J, Lewis C, Kahn CR** 2006 Evidence for a role of developmental genes in the origin of obesity and body fat distribution. Proc Natl Acad Sci U S A 103:6676-6681
12. **Niesler CU, Siddle K, Prins JB** 1998 Human preadipocytes display a depot-specific susceptibility to apoptosis. Diabetes 47:1365-1368
13. **Van Harmelen V, Rohrig K, Hauner H** 2004 Comparison of proliferation and differentiation capacity of human adipocyte precursor cells from the omental and subcutaneous adipose tissue depot of obese subjects. Metabolism 53:632-637
14. **Boden G, Duan X, Homko C, Molina EJ, Song W, Perez O, Cheung P, Merali S** 2008 Increase in endoplasmic reticulum stress-related proteins and genes in adipose tissue of obese, insulin-resistant individuals. Diabetes 57:2438-2444

15. **Ahmed M, Neville MJ, Edelmann MJ, Kessler BM, Karpe F** 2009 Proteomic Analysis of Human Adipose Tissue After Rosiglitazone Treatment Shows Coordinated Changes to Promote Glucose Uptake. Obesity (Silver Spring)
16. **Perez-Perez R, Ortega-Delgado FJ, Garcia-Santos E, Lopez JA, Camafeita E, Ricart W, Fernandez-Real JM, Peral B** 2009 Differential Proteomics of Omental and Subcutaneous Adipose Tissue Reflects Their Unalike Biochemical and Metabolic Properties. J Proteome Res 8:1682-93
17. **van Beek EA, Bakker AH, Kruyt PM, Hofker MH, Saris WH, Keijer J** 2007 Intra- and interindividual variation in gene expression in human adipose tissue. Pflugers Arch 453:851-861
18. **Fukuhara A, Matsuda M, Nishizawa M, Segawa K, Tanaka M, Kishimoto K, Matsuki Y, Murakami M, Ichisaka T, Murakami H, Watanabe E, Takagi T, Akiyoshi M, Ohtsubo T, Kihara S, Yamashita S, Makishima M, Funahashi T, Yamanaka S, Hiramatsu R, Matsuzawa Y, Shimomura I** 2005 Visfatin: a protein secreted by visceral fat that mimics the effects of insulin. Science 307:426-430
19. **Tan BK, Adya R, Farhatullah S, Lewandowski KC, O'Hare P, Lehnert H, Randeva HS** 2008 Omentin-1, a novel adipokine, is decreased in overweight insulin-resistant women with polycystic ovary syndrome: ex vivo and in vivo regulation of omentin-1 by insulin and glucose. Diabetes 57:801-8.
20. **Schaffler A, Neumeier M, Herfarth H, Furst A, Scholmerich J, Buchler C** 2005 Genomic structure of human omentin, a new adipocytokine expressed in omental adipose tissue. Biochim Biophys Acta 1732:96-102
21. **Berndt J, Kloting N, Kralisch S, Kovacs P, Fasshauer M, Schon MR, Stumvoll M, Bluher M** 2005 Plasma visfatin concentrations and fat depot-specific mRNA expression in humans. Diabetes 54:2911-2916
22. **Garg A, Agarwal AK** 2009 Lipodystrophies: Disorders of adipose tissue biology. Biochim Biophys Acta 1791:507-513
23. **Miranda M, Chacon MR, Gutierrez C, Vilarrasa N, Gomez JM, Caubet E, Megia A, Vendrell J** 2008 LMNA mRNA expression is altered in human obesity and type 2 diabetes. Obesity (Silver Spring) 16:1742-1748
24. **Lelliott CJ, Logie L, Sewter CP, Berger D, Jani P, Blows F, O'Rahilly S, Vidal-Puig A** 2002 Lamin expression in human adipose cells in relation to anatomical site and differentiation state. J Clin Endocrinol Metab 87:728-734
25. **Wojtanik KM, Edgemon K, Viswanadha S, Lindsey B, Haluzik M, Chen W, Poy G, Reitman M, Londos C** 2009 The role of LMNA in adipose: a novel mouse model of lipodystrophy based on the Dunnigan-type familial partial lipodystrophy mutation. J Lipid Res 50:1068-1079
26. **Lloyd DJ, Trembath RC, Shackleton S** 2002 A novel interaction between lamin A and SREBP1: implications for partial lipodystrophy and other laminopathies. Hum Mol Genet 11:769-777
27. **Louvet-Vallee S** 2000 ERM proteins: from cellular architecture to cell signaling. Biol Cell 92:305-316
28. **Barreiro O, Yanez-Mo M, Serrador JM, Montoya MC, Vicente-Manzanares M, Tejedor R, Furthmayr H, Sanchez-Madrid F** 2002 Dynamic interaction of VCAM-1 and ICAM-1 with moesin and ezrin in a novel endothelial docking structure for adherent leukocytes. J Cell Biol 157:1233-1245
29. **Koss M, Pfeiffer GR, 2nd, Wang Y, Thomas ST, Yerukhimovich M, Gaarde WA, Doerschuk CM, Wang Q** 2006 Ezrin/radixin/moesin proteins are

phosphorylated by TNF-alpha and modulate permeability increases in human pulmonary microvascular endothelial cells. J Immunol 176:1218-1227

30. **Lim S, Ryu J, Shin JA, Shin MJ, Ahn YK, Kim JJ, Han KH** 2009 Tumor Necrosis Factor-{alpha} Potentiates RhoA-Mediated Monocyte Transmigratory Activity In Vivo at a Picomolar Level. Arterioscler Thromb Vasc Biol

31. **Duffaut C, Zakaroff-Girard A, Bourlier V, Decaunes P, Maumus M, Chiotasso P, Sengenes C, Lafontan M, Galitzky J, Bouloumie A** 2009 Interplay between human adipocytes and T lymphocytes in obesity: CCL20 as an adipochemokine and T lymphocytes as lipogenic modulators. Arterioscler Thromb Vasc Biol 29:1608-1614

32. **O'Rourke RW, Metcalf MD, White AE, Madala A, Winters BR, Maizlin, II, Jobe BA, Roberts CT, Jr., Slifka MK, Marks DL** 2009 Depot-specific differences in inflammatory mediators and a role for NK cells and IFN-gamma in inflammation in human adipose tissue. Int J Obes (Lond)

33. **Harman-Boehm I, Bluher M, Redel H, Sion-Vardy N, Ovadia S, Avinoach E, Shai I, Kloting N, Stumvoll M, Bashan N, Rudich A** 2007 Macrophage infiltration into omental versus subcutaneous fat across different populations: effect of regional adiposity and the comorbidities of obesity. J Clin Endocrinol Metab 92:2240-2247

34. **Hotamisligil GS** 2006 Inflammation and metabolic disorders. Nature 444:860-867

35. **Nishimura S, Manabe I, Nagasaki M, Eto K, Yamashita H, Ohsugi M, Otsu M, Hara K, Ueki K, Sugiura S, Yoshimura K, Kadowaki T, Nagai R** 2009 CD8+ effector T cells contribute to macrophage recruitment and adipose tissue inflammation in obesity. Nat Med 15:914-920

36. **Linial M, Miller K, Scheller RH** 1989 VAT-1: an abundant membrane protein from Torpedo cholinergic synaptic vesicles. Neuron 2:1265-1273

37. **Kreier F, Kap YS, Mettenleiter TC, van Heijningen C, van der Vliet J, Kalsbeek A, Sauerwein HP, Fliers E, Romijn JA, Buijs RM** 2006 Tracing from fat tissue, liver, and pancreas: a neuroanatomical framework for the role of the brain in type 2 diabetes. Endocrinology 147:1140-1147

38. **Marchitti SA, Brocker C, Stagos D, Vasiliou V** 2008 Non-P450 aldehyde oxidizing enzymes: the aldehyde dehydrogenase superfamily. Expert Opin Drug Metab Toxicol 4:697-720

39. **Bonet ML, Ribot J, Felipe F, Palou A** 2003 Vitamin A and the regulation of fat reserves. Cell Mol Life Sci 60:1311-1321

40. **Adams M, Montague CT, Prins JB, Holder JC, Smith SA, Sanders L, Digby JE, Sewter CP, Lazar MA, Chatterjee VK, O'Rahilly S** 1997 Activators of peroxisome proliferator-activated receptor gamma have depot-specific effects on human preadipocyte differentiation. J Clin Invest 100:3149-3153

41. **Tchkonia T, Giorgadze N, Pirtskhalava T, Thomou T, DePonte M, Koo A, Forse RA, Chinnappan D, Martin-Ruiz C, von Zglinicki T, Kirkland JL** 2006 Fat depot-specific characteristics are retained in strains derived from single human preadipocytes. Diabetes 55:2571-2578

Figure 1

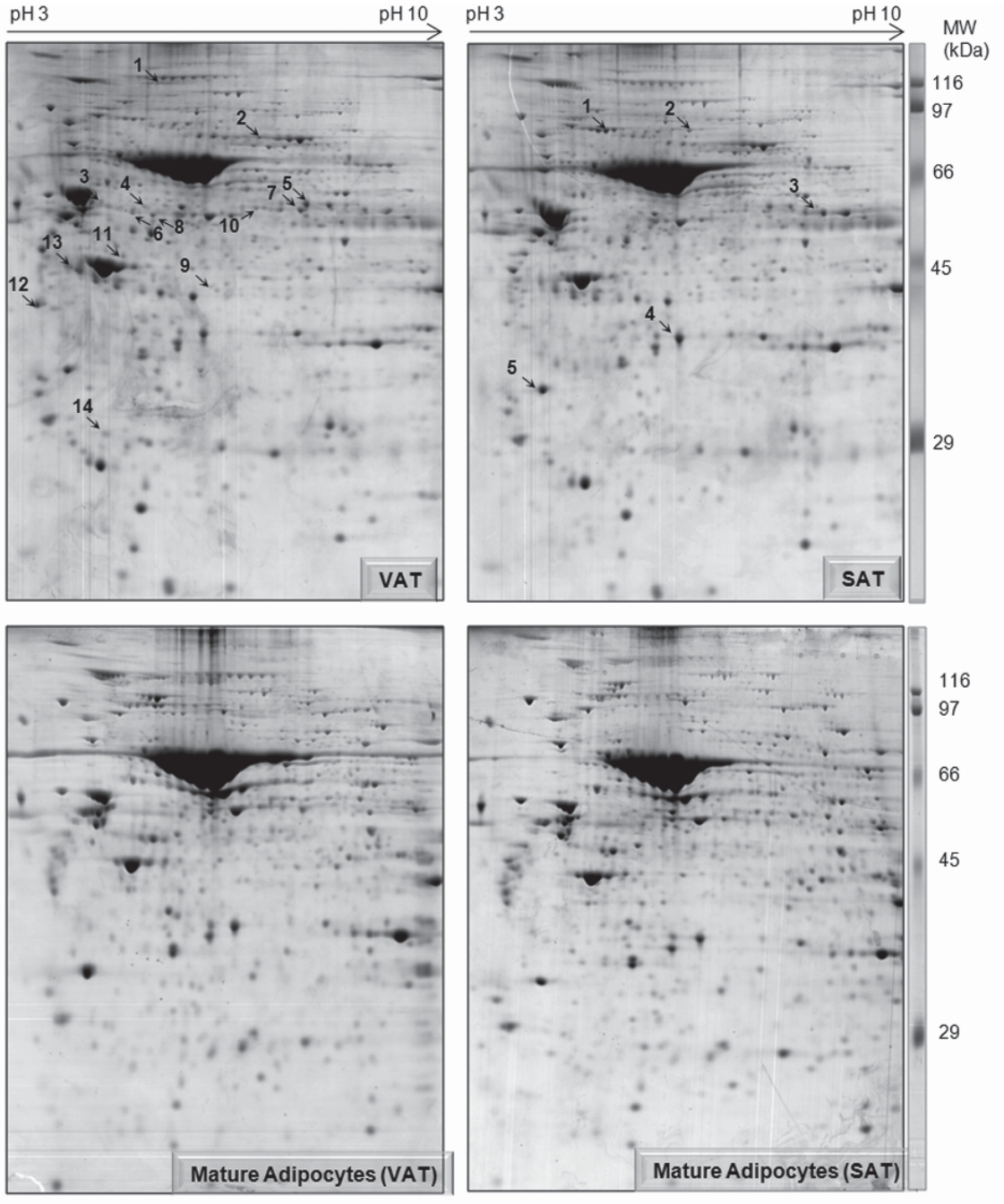
pH 3
pH 10
pH 3
pH 10
MW (kDa)
116
97
66
45
29
1
2
3
4
5
6
7
8
9
10
11
12
13
14
VAT
SAT
116
97
66
45
29
Mature Adipocytes (VAT)
Mature Adipocytes (SAT)

Figure 2

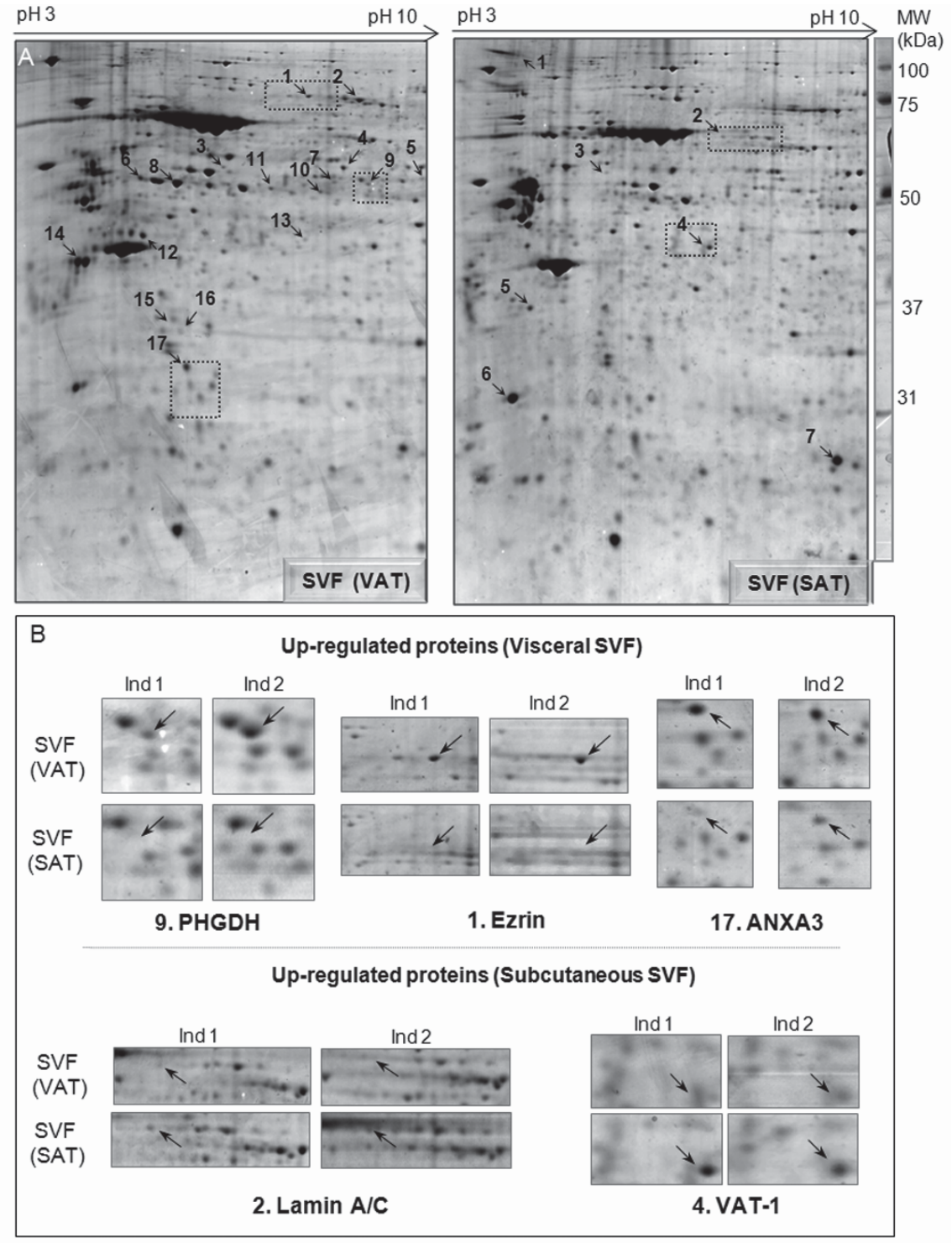
pH 3
pH 10
A
SVF (VAT)
SVF (SAT)
MW (kDa)
100
75
50
37
31
B
Up-regulated proteins (Visceral SVF)
Ind 1
Ind 2
SVF (VAT)
SVF (SAT)
9. PHGDH
1. Ezrin
17. ANXA3
Up-regulated proteins (Subcutaneous SVF)
2. Lamin A/C
4. VAT-1

Figure 3

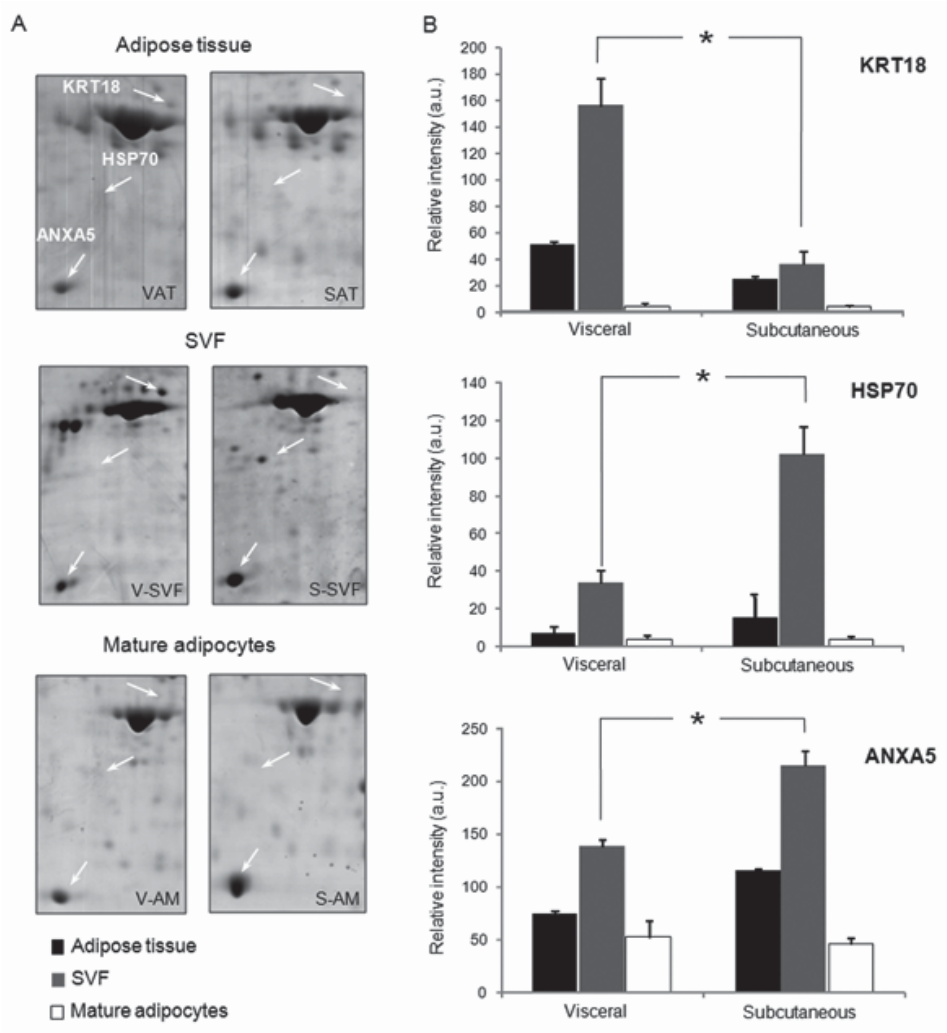
A
Adipose tissue
KRT18
HSP70
ANXA5
VAT
SAT
SVF
V-SVF
S-SVF
Mature adipocytes
V-AM
S-AM
Adipose tissue
SVF
Mature adipocytes
B
KRT18
HSP70
ANXA5
Relative intensity (a.u.)
Visceral
Subcutaneous
*

Figure 4

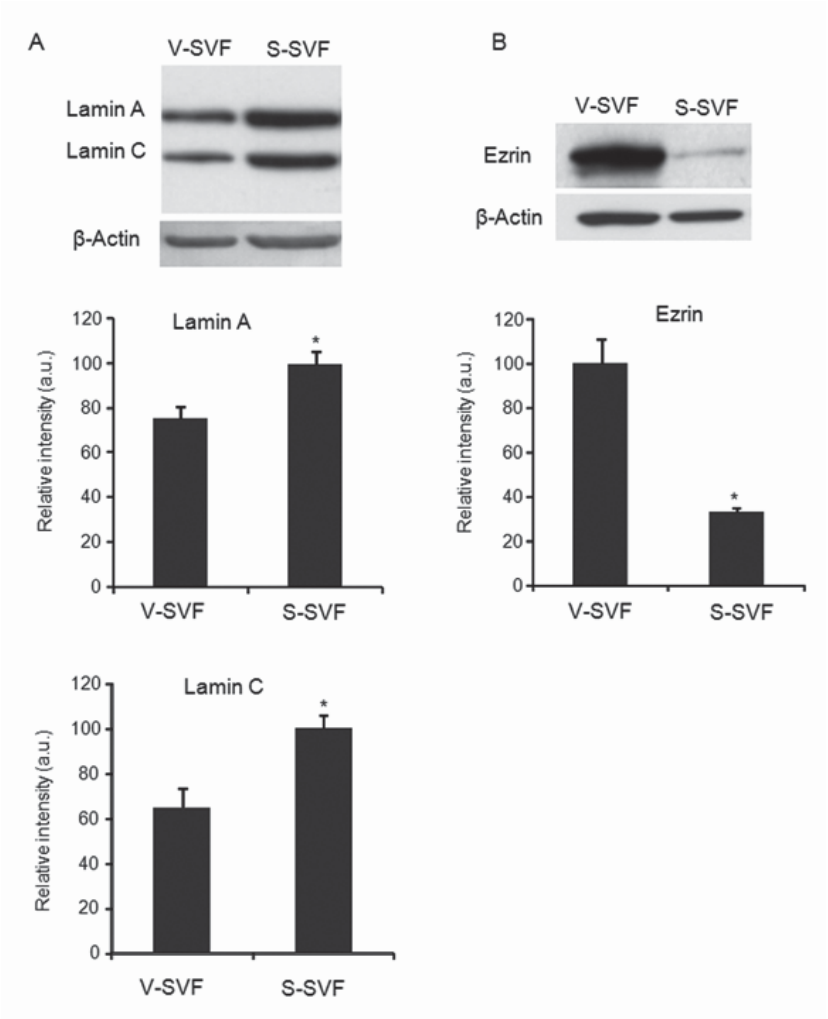
A
V-SVF
S-SVF
Lamin A
Lamin C
β-Actin
B
V-SVF
S-SVF
Ezrin
β-Actin
Lamin A
Relative intensity (a.u.)
120
100
80
60
40
20
0
V-SVF
S-SVF
*
Ezrin
Relative intensity (a.u.)
120
100
80
60
40
20
0
V-SVF
S-SVF
*
Lamin C
Relative intensity (a.u.)
120
100
80
60
40
20
0
V-SVF
S-SVF
*

Figure 5

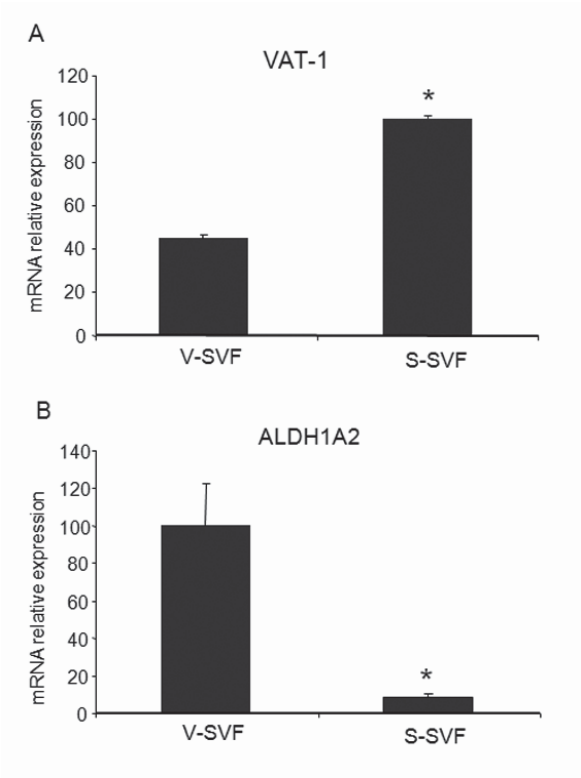
A
VAT-1
mRNA relative expression
120
100
80
60
40
20
0
*
V-SVF
S-SVF
B
ALDH1A2
mRNA relative expression
140
120
100
80
60
40
20
0
*
V-SVF
S-SVF